How to cite: *Angew. Chem. Int. Ed.* **2022,** *61,* e202207998
International Edition: doi.org/10.1002/anie.202207998
German Edition: doi.org/10.1002/ange.202207998

Soft Matter

Membrane Manipulation of Giant Unilamellar Polymer Vesicles with a Temperature-Responsive Polymer

Marina de Souza Melchiors, Tsvetomir Ivanov, Iain Harley, Claudia Sayer, Pedro H. H. Araújo, Lucas Caire da Silva, Calum T. J. Ferguson,* and Katharina Landfester**

Abstract: Understanding the complex behavior and dynamics of cellular membranes is integral to gain insight into cellular division and fusion processes. Bottom-up synthetic cells are as a platform for replicating and probing cellular behavior. Giant polymer vesicles are more robust than liposomal counterparts, as well as having a broad range of chemical functionalities. However, the stability of the membrane can prohibit dynamic processes such as membrane phase separation and division. Here, we present a method for manipulating the membrane of giant polymersomes using a temperature responsive polymer. Upon elevation of temperature deformation and phase separation of the membrane was observed. Upon cooling, the membrane relaxed and became homogeneous again, with infrequent division of the synthetic cells.

Cellular division is an integral process where every living cell found on Earth today originates from a pre-existing living cell.[1,2] Cells have evolved to possess complex machinery capable of reproducibly dividing cells, transferring information from one cell to the next. Understanding the processes from nature has long been targeted through the replication and mimicry in a minimalistic system. Bottom-up assembly of synthetic cells provides a platform to investigate the complex nature of cells. To date, various platforms have been developed including, liposomes,[3] polymersomes,[4] droplets,[5] and micelles.[6] The manipulation of the membranes of synthetic cells has often been targeted as a method to induce conformational changes in shape. Liposomal systems have a very dynamic membrane and, therefore, much of the initial work has been undertaken with liposomal membranes, where phase separation and division have been shown.[7–10] Giant unilamellar polymer vesicles (GUVs) are more challenging due to the composition of the membrane, where the polymers used have higher molecular weights and are therefore less dynamic. The formation of patchy polymer GUVs has been reported, by membrane phase separation upon formation.[11] However, triggered membrane manipulation and division of polymer GUVs have remained major challenges.

Polymer GUVs are cell-sized vesicles (10–100 μm) made of amphiphilic copolymers. These polymer vesicles, also known as polymersomes, are formed by the spontaneous self-assembly of the copolymers, driven by the presence of a hydrophilic and a hydrophobic block in the same polymer chain.[12,13] The resulting vesicular structure is characterized by a single bilayer, like that of natural lipids. Because of their similarity to the cell membrane, polymer GUVs are used as biomimetic model compartments for biophysical studies and to create cell-like systems that mimic the structure and function of living cells.[14] GUVs made from polymers are characterized by high mechanical stability and the wide chemical and structural variability that can be achieved by synthetic polymer chemistry. Their chemical versatility allows the preparation of GUVs whose properties can be easily tuned, e.g., responsiveness to stimuli, interfacial chemistry, and general biophysical behavior.[15,16] Due to the large size of polymer GUVs, dynamic processes such as the increase in membrane area (growth), changes in morphology, and division of vesicles can be easily observed using optical microscopy. These are examples of membrane manipulation events that can be used to control the structural properties of polymer vesicles and the compartmentalized systems made from them.[17] Aside from applications in the development of advanced cell-like systems, the study of membrane manipulation in polymer GUVs can also help researchers gain a better understanding of the driving

[*] Dr. M. de Souza Melchiors, T. Ivanov, I. Harley, Dr. L. Caire da Silva, Dr. C. T. J. Ferguson, Prof. Dr. K. Landfester
Department of Physical Chemistry of Polymers, Max Planck Institute for Polymer Research
Ackermannweg 10, 55128 Mainz (Germany)
E-mail: silva@mpip-mainz.mpg.de
ferguson@mpip-mainz.mpg.de
landfester@mpip-mainz.mpg.de

Dr. M. de Souza Melchiors, Prof. Dr. C. Sayer, Prof. Dr. P. H. H. Araújo
Department of Chemical Engineering and Food Engineering, Federal University of Santa Catarina
P.O. Box 476, 88040-900, Florianópolis-SC (Brazil)

Dr. C. T. J. Ferguson
School of Chemistry, University of Birmingham
Edgbaston, Birmingham, B15 2TT (UK)
E-mail: c.ferguson.1@bham.ac.uk

forces that lead to membrane manipulation in natural cells. However, there are few studies in the literature on the manipulation of biomembranes with polymer GUVs.[18,19] This is because the division and shape control of polymer vesicles are difficult to achieve due to the robust nature of polymer membranes.

Herein, we report a strategy for the membrane manipulation of polymer GUVs. A temperature-responsive diblock copolymer, poly(N,N-dimethylacrylamide)-block-poly(N-isopropylacrylamide) (PDMA-*b*-PNIPAM), was incorporated into the membrane of non-responsive poly(butadiene)-*block*-poly(ethylene oxide) (PBD-*b*-PEO) vesicles, during formation via a double emulsification method (Figure S1).[20] Initially, the system was formed at room temperature, below the lower critical solution temperature of PNIPAM. Upon elevating the temperature, the NIPAM block is no longer solvated and phase separates to form polymeric structures within the membrane (Scheme 1). This change in colloidal properties induced mechanical fluctuations in the polymer membrane creating morphological changes.

Furthermore, upon cooling of the system, the PDMA-*b*-PNIPAM relaxes to its original solvation state increasing its volume fraction, inducing further modulation of the membrane, including division. The diblock copolymer, PDMA-*b*-PNIPAM, was incorporated into the membrane of GUVs. The temperature responsive diblock copolymers (TRC) consisting of $PDMA_{30}$-b-$PNIPAM_{200}$-BODIPY were synthesized using reversible addition-fragmentation chain-transfer (RAFT) mediated by polymerization-induced self-assembly (PISA) as previously reported.[21] Here, a poly(N,N-dimethylacrylamide) (PDMA) macro chain transfer agent was initially formed using 4-((((2-carboxyethyl) thio)carbonothioyl)thio)-4-cyanopentanoic acid and then chain extended with the temperature responsive monomer N-isopropylacrylamide (NIPAM; Figure 1a). Furthermore, to enable easy detection of the temperature responsive polymer, a BODIPY methacrylate monomer was incorporated into the polymer.

At ambient temperature, the synthesized temperature responsive copolymer (TRC) is a translucent solution with a fully dissolved polymer. Upon elevation of the temperature, the TRC formed polymeric aggregates between 200 and 250 nm in diameter, as determined by light scattering at 90°

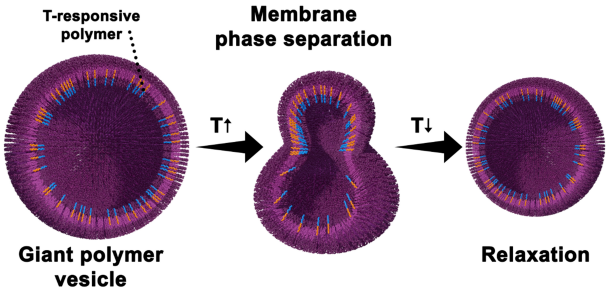

Scheme 1. Overview of membrane manipulation in polymersome model by heating and cooling cycles.

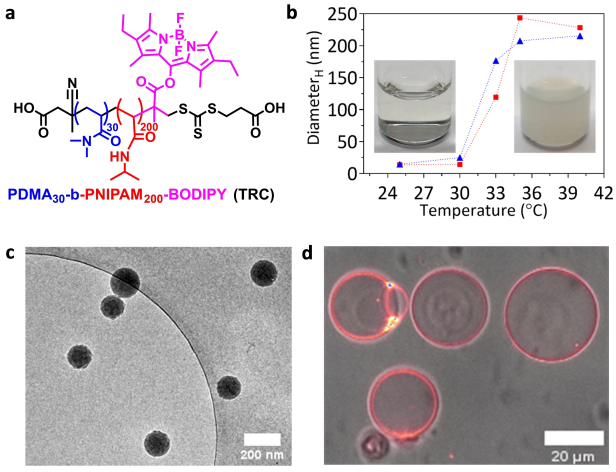

Figure 1. a) Structure; b) Z-average particle size as a function of temperature between 25 °C and 40 °C, the blue line corresponds to the cooling cycle, while the red corresponds to the heating cycle; c) cryo-TEM of $PDMA_{30}$-*b*-$PNIPAM_{200}$; d) Optical microscopy observation showing incorporation of $PDMA_{30}$-*b*-$PNIPAM_{200}$-BODIPY into PBD_{51}-*b*-PEO_{27} polymersome at 28 °C.

(Figure 1b). PNIPAM is a thermoresponsive polymer that displays a lower critical solution temperature (LCST) behavior with a reported coil-globule transition at around 32 °C, similar to what was observed in this study.[22] To investigate the morphology of the temperature induced self-assembly, cryogenic transmission electron microscopy (cryo-TEM) was used (Figure 1c). Cryo-TEM revealed submicron size aggregates at a dry state with well-defined spherical morphology. To verify the incorporation of the TRC into the membrane of the GUVs, an image was obtained at 28 °C using confocal laser microscopy (Figure 1d).

The fluorescence from BODIPY showed that the temperature responsive polymer was incorporated into the membrane of the PBD-*b*-PEO GUV (Figure 1d). At 28 °C, below the LCST, the TRC is readily solvated in water. Therefore, TRC was expected to be confined to the inner volume of vesicles and barely present in the vesicle membrane. Conversely, in the direction of minimizing free energy the TRC migrated into the bilayer as the interaction with PBD-PEO was favored compared to the full solvation. Thus, even in its water-soluble form the polymer-polymer interactions between the TRC the PBD-*b*-PEO membrane were favored due to the surface activity of the TRC. Indeed, interfacial tension measurements of the TRC in water + PBD-PEO in toluene showed that the TRC is surface-active, which is consistent with the interaction of TRC with the PBD-PEO membrane below the LCST (See Table S3). Moreover, the TRC is not only solubilized in water but can readily be solvated by a range of more polar solvents (Figure S4).

The effect of temperature on the morphology of polymersomes containing the TRC was investigated by confocal microscopy (Figure 2a). At ambient temperature (28 °C) and below the LCST, the polymersomes had a spherical shape and exhibited the fluorescently labelled

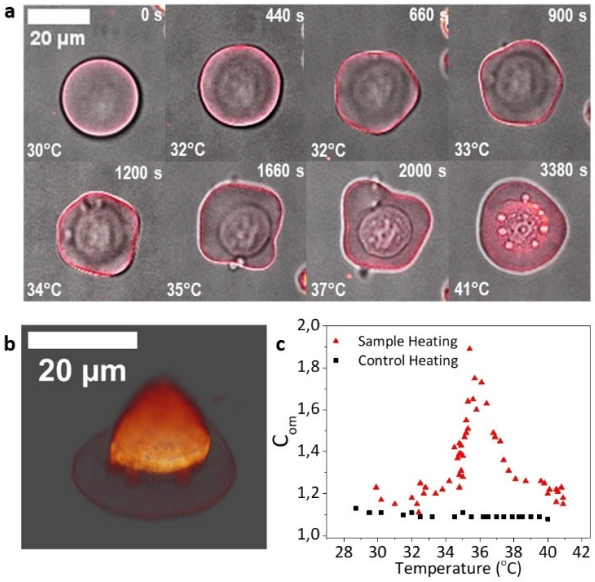

Figure 2. Membrane manipulation process in a polymersome observed by confocal microscopy, $PDMA_{30}$-*b*-$PNIPAM_{200}$-BODIPY:$PDMA_{30}$-*b*-$PNIPAM_{200}$ (1:100) (90 mg mL^{-1}) and membrane PBD_{51}-*b*-PEO_{27} +10 mol% cholesterol, a) heating cycle 28 °C to 40 °C, b) 3D images at 40 °C; c) temperature dependent change in compactness of a single polymersome in one independent experiment. The control heating involves a polymersome composed of only PBD_{51}-*b*-PEO_{27} + 10 mol% cholesterol.

TRC in the membrane as expected. The vesicle shape did not change during the first 430 s (Supplementary Video 1) at room temperature. After heating to 34 °C, slightly above the LCST, the polymersomes deformed significantly, as shown in Figure 2a. Additionally, the gradual development of a distinct area on the polymeric GUV indicated phase separation between the two distinct polymers. Closer inspection showed that the deformation led to a non-spherical shape with an increased cross-sectional perimeter which is consistent with the lateral expansion of the polymersome membrane (Figure S12.). As the membrane heats up, it continues to deform, with the phase-separated region becoming more prominent. The lower the hydrophilicity of the TRC, the greater the tendency to integrate with the membrane. The high fluorescence intensity within the phase-separated area (Figure 2b) demonstrated that a heterogeneous membrane is being formed where the TRC aggregates. The driving force for the phase separation emerges from the differences in the chain lengths of the hydrophobic blocks (200 units of NIPAM vs 51 units of BD) and the chemical nature of the monomers in the polymer membrane (NIPAM vs BD), which can be explained by the improved polymer-polymer interaction of NIPAM above LCST, where the system reorganizes itself to maximize these NIPAM-NIPAM interactions compared to NIPAM-BD. The mismatch contributes to the unfavourable mixing of the two blocks, which leads to phase separation.[23] Similar segregation behavior was also observed in hybrid polymer/lipid vesicles.[11,24]

Figure 2b shows a cross section from a 3D reconstruction of a polymersome obtained by confocal laser microscopy during the phase separation at 41 °C. The image shows two distinct regions: the membrane that defines the perimeter of the cross section and the phase separated area at the center of the polymersome surface. The phase separated dome shows a higher signal intensity that is consistent with the higher concentration of the TRC compared to the bulk of the polymersome. The morphology observed in this temperature responsive system is similar to that observed in phase separated droplets, where acorn shaped structures are observed.[25–27] Polymer/polymer phase separation in vesicles was also reported by researchers investigating the effect of polymer chain incompatibility on the surface topology of polymersomes.[11,28]

The extent of change in vesicle shape as a function of temperature was analysed in terms of changes in compactness (C_{om}) (Figure 2c). Compactness was calculated as the ratio between the square of the perimeter and 4π multiplied by the cross-sectional area of polymersomes obtained from confocal micrographs (Figure S2). C_{om} is minimal (1.0) for a perfect circle and increases with deviations from this shape.[29] Figure 2c shows that C_{om} dramatically increases at 34 °C, peaking at 36 °C at 1.9 before returning to a compactness of 1.2 at 40 °C. The sharp increase in the C_{om} coincided with the phase separation of TRC in the PBD-PEO membrane. The return to a spherical shape after the peak in C_{om} is consistent with the relaxation of the membrane as it incorporates the TRC as an integral part of the vesicle membrane. The sharp increase in C_{om} can be explained by the high molecular weight of the TRC, which restricts its mobility within the vesicle membrane. As TRC is integrated into the membrane, low mobility regions rich in the high molecular weight TRC need a longer time to relax. As soon as the heterogeneous membrane relaxes, it regains its spherical shape (low C_{om}). It is important to note that C_{om} corresponds to a 2D description of the vesicles, which could obscure finer details of the behavior

The observed changes in vesicle shape did not occur when the concentration of the TRC was reduced from 90 mg mL^{-1} to 30 mg mL^{-1} (Figure S8). Therefore, a relatively large concentration of the TRC must be initially present inside the vesicles in order to produce the morphological changes. Moreover, when the molecular weight of the PBD-PEO polymer was reduced from 5900 g mol^{-1} to 1800 g mol^{-1} while TRC was kept at 90 mg mL^{-1}, no changes in vesicle shape were observed (Figure S9). The lower Mw of PBD-PEO is expected to result in a more malleable vesicle membrane that can relax faster without sharp changes in compactness.

Due to the reversible temperature-dependent nature of TRC, the changes observed during heating were expected to be reversed at cooling. In fact, the reversibility was confirmed as shown in Figure 3. Surprisingly, during the gradual return of the vesicle to the low temperature state, a bud formed at t_0 + 5030s and continued to elongate until a daughter vesicle was produced (Figure 3a, arrows). This phenomenon can be explained by the heterogeneity of the membrane during the heating-cooling cycle, which leads to

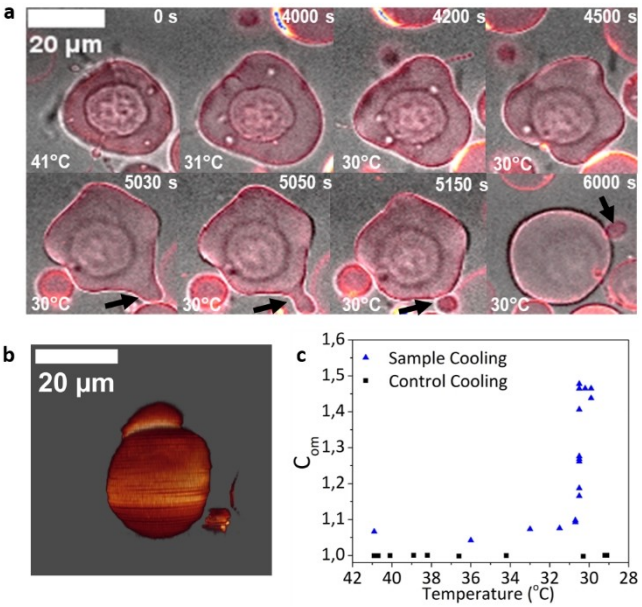

Figure 3. Self-division process in a polymersome observed by using confocal microscopy, $PDMA_{30}$-*b*-$PNIPAM_{200}$-BODIPY:$PDMA_{30}$-b-$PNIPAM_{200}$ (1:100) (90 mg mL^{-1}) and membrane PBD_{51}-b-PEO_{27} + 20 mol% Cholesterol, a) cooling cycle 40 °C to 28 °C, b) 3D images at 28 °C; c) the time courses of the change in compactness of "single polymersome" in one independent experiment. The control cooling involves a polymersome composed of only PBD_{51}-*b*-PEO_{27} + 20 mol% cholesterol.

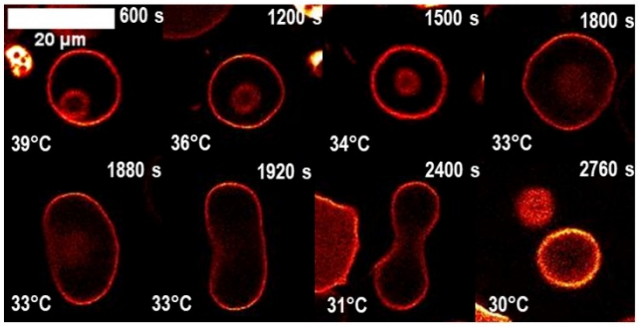

Figure 4. Self-division in a polymersome during cooling from 39 °C to 28 °C observed by confocal microscopy. $PDMA_{30}$-b-$PNIPAM_{200}$-BODIPY:$PDMA_{30}$-b-$PNIPAM_{200}$ (1:100) (90 mg mL^{-1}) and membrane PBD_{51}-b-PEO_{27}.

the formation of domain boundaries with increased tension, causing the relaxation of the system by budding and vesicle splitting.[30,31] The 3D reconstruction of the polymersome during the cooling cycle at low temperature is shown in Figure 3b. It shows that the polymersome returned to its initial size (spherical morphology, low C_{om}) with the fluorescently labelled temperature responsive polymer also located in the membrane indicating the reversible nature of the process. Formation of a daughter vesicle caused a corresponding increase in C_{om} (Figure 3c) at a determined temperature below LCST. The C_{om} had a significant rise at 30 °C corresponding to times from 4000 s to 6000 s.

The relaxation of the membrane from elevated temperature to ambient temperature produced a diverse range of effects. Here, multiple incidences of division were observed, but the majority of polymersomes appeared to have asymmetric membrane deformation without division (Figure 4 and S10). Other effects, such as the formation of filaments on the surface of the polymersomes, were also observed, suggesting a secondary mechanism by which the membrane may eliminate excess polymer during temperature cycling (Figure S11).

Cholesterol was added in some experiments to increase the stability of the vesicles during formation and during the experiments. Cholesterol is known for its influence on the stability and organization of the membrane in liposomes and can change physical characteristics, such as decreasing fluidity and influencing permeability.[32] However, the net effect depends on the temperature and membrane composition. Figure S5–S7 shows the results of control experiments with 0–20 mol% of cholesterol in vesicles lacking the TRC. As expected, no membrane manipulation occurred, indicating that cholesterol was not responsible for the membrane manipulation. Samples containing TRC but no cholesterol showed significant changes in vesicle shape. The degree of manipulation was enhanced when the concentration of cholesterol was increased. Interestingly, no differences were observed in samples containing 10 or 20 mol% cholesterol, suggesting that the maximum effect was achieved after 10 % mol (Figure S14). Permeability tests were performed to evaluate the effect of cholesterol on membrane permeability. Dye leakage measurements did not indicate membrane permeabilization in the polymersomes as a function of cholesterol content (Figures S15–S18).

To conclude, a new approach to mimic biomembrane manipulation using a polymersome model was presented. Reversible integration of TRC into the membrane of PBD-PEO vesicles driven by temperature cycling resulted in changes in vesicle shape and occasional division of vesicles. The strategies and materials developed in this study can be used to create compartmentalized systems that can mimic the adaptive properties of biomembranes. This expands the use of polymersomes in various fields where adaptability is required, such as cell-like microreactors, biosensors, and drug delivery vehicles. Further studies to determine the exact processes that lead to the division are underway and will be presented in future work.

Acknowledgements

The authors are grateful to Anke Kaltbeitzel from Max Planck Institute for Polymer Research for her kind assistance with the confocal microscope images, Ute Heinz, and Sandra Seywald for the GPC measurements, and Petra Räder for TGA and DSC measurements. We also appreciate the financial support for this work from Coordenação de Aperfeiçoamento de Pessoal de Nível Superior (CAPES), and Conselho Nacional de Desenvolvimento Científico e Tecnológico (CNPq) Processo n° 201470/2019-5 for the

scholarship to Dr. M. S. Melchiors. This work is part of the research conducted within the Max Planck Consortium for Synthetic Biology (MaxSynBio) jointly funded by the Federal Ministry of Education and Research of Germany (BMBF) and the Max Planck Society. I. H. gratefully acknowledges the H2020 Marie Curie Actions Fellowship of the European Commission (ITN SUPERCOL, Grant Agreement 860914). Open Access funding enabled and organized by Projekt DEAL.

Conflict of Interest

The authors declare no conflict of interest.

Data Availability Statement

The data that support the findings of this study are available from the corresponding author upon reasonable request.

Keywords: Biomimetic Membranes · Block Copolymers · Membrane Manipulation · Phase Separation · Polymersomes

[1] R. Virchow, *Die Cellularpathologie in Ihrer Begründung Auf Physiologische Und Pathologische Gewebelehre. Zwanzig Vorlesungen Gehalten Während Der Monate Februar, März Und April 1858 Im Pathologischen Institute Zu Berlin*, Berlin, A. Hirschwald, **1858**.
[2] F. V. Raspail, *Ann. Sci. Nat.* **1825**, *6*, 224–239.
[3] S. Deshpande, Y. Caspi, A. E. C. Meijering, C. Dekker, *Nat. Commun.* **2016**, *7*, 10447.
[4] B. M. Discher, Y.-Y. Won, D. S. Ege, J. C. M. Lee, F. S. Bates, D. E. Discher, D. A. Hammer, *Science* **1999**, *284*, 1143–1146.
[5] M. Weiss, J. P. Frohnmayer, L. T. Benk, B. Haller, J.-W. Janiesch, T. Heitkamp, M. Börsch, R. B. Lira, R. Dimova, R. Lipowsky, E. Bodenschatz, J.-C. Baret, T. Vidakovic-Koch, K. Sundmacher, I. Platzman, J. P. Spatz, *Nat. Mater.* **2018**, *17*, 89–96.
[6] Y. Geng, P. Dalhaimer, S. Cai, R. Tsai, M. Tewari, T. Minko, D. E. Discher, *Nat. Nanotechnol.* **2007**, *2*, 249–255.
[7] Y. Dreher, K. Jahnke, M. Schröter, K. Göpfrich, *Nano Lett.* **2021**, *21*, 5952–5957.
[8] Y. Dreher, K. Jahnke, E. Bobkova, J. P. Spatz, K. Göpfrich, *Angew. Chem. Int. Ed.* **2021**, *60*, 10661–10669; *Angew. Chem.* **2021**, *133*, 10756–10764.
[9] R. Lipowsky, *Adv. Colloid Interface Sci.* **2022**, *301*, 102613.
[10] M. Andes-Koback, C. D. Keating, *J. Am. Chem. Soc.* **2011**, *133*, 9545–9555.
[11] E. Rideau, F. R. Wurm, K. Landfester, *Small* **2020**, *16*, 1905230.
[12] E. C. dos Santos, A. Angelini, D. Hürlimann, W. Meier, C. G. Palivan, *Chemistry* **2020**, *2*, 470–489.
[13] D. E. Discher, F. Ahmed, *Annu. Rev. Biomed. Eng.* **2006**, *8*, 323–341.
[14] M. Jiménez, A. Martos, E. J. Cabré, A. Raso, G. Rivas, *Environ. Microbiol.* **2013**, *15*, 3158–3168.
[15] M. Fauquignon, E. Ibarboure, S. Carlotti, A. Brûlet, M. Schmutz, J.-F. Le Meins, *Polymers* **2019**, *11*, 2013.
[16] A. Peyret, E. Ibarboure, A. Tron, L. Beauté, R. Rust, O. Sandre, N. D. McClenaghan, S. Lecommandoux, *Angew. Chem. Int. Ed.* **2017**, *56*, 1566–1570; *Angew. Chem.* **2017**, *129*, 1588–1592.
[17] C. Guindani, L. C. Silva, S. Cao, T. Ivanov, K. Landfester, *Angew. Chem. Int. Ed.* **2022**, *61*, e202110855; *Angew. Chem.* **2022**, *134*, e202110855.
[18] J. Sun, S. J. Rijpkema, J. Luan, S. Zhang, D. A. Wilson, *Nat. Commun.* **2021**, *12*, 2235.
[19] A. C. Greene, I. M. Henderson, A. Gomez, W. F. Paxton, V. VanDelinder, G. D. Bachand, *PLoS One* **2016**, *11*, e0158729.
[20] M. Houbrechts, L. Caire da Silva, A. Ethirajan, K. Landfester, *Soft Matter* **2021**, *17*, 4942–4948.
[21] Y. Xu, Y. Li, X. Cao, Q. Chen, Z. An, *Polym. Chem.* **2014**, *5*, 6244–6255.
[22] J. Chen, Q. Su, R. Guo, J. Zhang, A. Dong, C. Lin, J. Zhang, *Macromol. Chem. Phys.* **2017**, *218*, 1700166.
[23] G. H. Fredrickson, A. J. Liu, F. S. Bates, *Macromolecules* **1994**, *27*, 2503–2511.
[24] M. Chemin, P. M. Brun, S. Lecommandoux, O. Sandre, J. F. Le Meins, *Soft Matter* **2012**, *8*, 2867–2874.
[25] A. Misra, M. W. Urban, *Macromol. Rapid Commun.* **2010**, *31*, 119–127.
[26] Y. Wang, B.-H. Guo, X. Wan, J. Xu, X. Wang, Y.-P. Zhang, *Polymer* **2009**, *50*, 3361–3369.
[27] C. C. Campillo, A. P. Schröder, C. M. Marques, B. Pépin-Donat, *Soft Matter* **2008**, *4*, 2486–2491.
[28] J. Nam, P. A. Beales, T. K. Vanderlick, *Langmuir* **2011**, *27*, 1–6.
[29] M. A. S. Karal, S. Ahammed, V. Levadny, M. Belaya, M. K. Ahamed, M. Ahmed, Z. Bin Mahbub, A. K. M. A. Ullah, *Chem. Phys. Lipids* **2020**, *230*, 104916.
[30] C. Sanson, J.-F. Le Meins, C. Schatz, A. Soum, S. Lecommandoux, *Soft Matter* **2010**, *6*, 1722–1730.
[31] T. Baumgart, S. T. Hess, W. W. Webb, *Nature* **2003**, *425*, 821–824.
[32] J. R. Silvius, *Biochim. Biophys. Acta Biomembr.* **2003**, *1610*, 174–183.

Manuscript received: May 31, 2022
Accepted manuscript online: August 5, 2022
Version of record online: August 23, 2022